Geometrical and Electronic Structure of the Pt_7 Cluster: A Density Functional Study

Wei Quan Tian,[†] Maofa Ge,*[,‡,§] B. R. Sahu,[||] Dianxun Wang,[‡] Toshiki Yamada,[§] and Shinro Mashiko[§]

Department of Chemistry, University of British Columbia, 2036 Main Mall, Vancouver, BC, Canada, V6T 1Z1, Center of Molecular Science, Institute of Chemistry, Chinese Academy of Sciences, Beijing 100080, P. R. China, Department of Physics, University of Texas at Austin, Austin, Texas 78712-0264, and Communications Research Laboratory, Kansai Advanced Research Center, 588-2 Iwaoka, Kobe 651-2942, Japan

Received: January 13, 2004; In Final Form: February 20, 2004

We present a study on the structural and electronic properties of the Pt_7 cluster by using density functional theory within the generalized gradient approximation for the exchange and correlation. The structures, relative stabilities, and vibrational frequencies of various isomers are calculated and compared with the well-studied Au_7 cluster. The ground state of the Pt_7 cluster favors a three-dimensional geometry—two-dimensional local minima are not located—whereas for its neighbor, gold heptamer, a two-dimensional geometry is favored. The most stable isomer of Au_7 is found to be an edge-capped rhombus structure and an edge-capped tetrahedron structure is found to be the most stable three-dimensional local minimum. The ground state of the Pt_7 cluster is found to be a coupled tetragonal pyramid structure with the quintet state in contrast to a pentagonal bipyramid structure obtained by semiempirical molecular dynamics calculation. The natural orbital analysis shows that the overall charge transfer is from 6s to 5d orbitals in the Pt_7 cluster, whereas in Au_7 cluster it is from 5d to 6s. The molecular orbital picture shows that the bonding orbitals are due to the hybridization between 5d and 6s molecular orbitals in Pt_7 cluster, and the nonbonding and antibonding orbitals lie close to the highest occupied molecular orbital. This may be compared with the Au_7 electronic structure, where the nonbonding and antibonding orbitals mainly consists of 5d6s hybridized molecular orbitals.

I. Introduction

The intense studies on noble metal clusters and nanoparticles are motivated by their potential applications as building blocks for functional nanostructured materials, electronic devices, and nanocatalysts.[1] The structure and bonding characteristics of small metal clusters are quite interesting, as they also provide a tractable platform to comprehend the reactivity of small molecules on the metal surface and chemisorption.

Many experimental and theoretical works so far have been focused on small gold clusters,[2−8] and much less is known about the geometrical structures and energetics of small platinum clusters. Experimental studies on small pure Pt clusters are scarce. To the best of our knowledge, there are only some studies on Pt_2 by resonant two-photon ionization spectroscopy, vibrational spectroscopy, and dispersed fluorescence spectroscopy; negative ion photodetachment spectroscopic studies on Pt_2 and Pt_3; and collision-induced dissociation (CID) studies on Pt_n ($n = 2-5$).[9−14] On the theoretical side, there are two molecular dynamics (MD) simulations using different models and model potentials,[15,16] and there are also a few ab initio or density functional theory (DFT) studies on Pt_n ($n = 2-6$, 13, 55).[17−23]

Au was described as the "gold maximum" of relativistic effects.[23] The preference for a two-dimensional (2D) structure of small gold clusters was ascribed to relativistic effects causing strong hybridization of the atomic 5d and 6s orbitals, whereas small copper and silver clusters prefer a three-dimensional (3D) structure.[3] As gold's neighbor, platinum also has a strong relativistic effect, for example, for bond length contractions.[24] The different electronic configuration of gold ($5d^{10}6s^1$) and platinum ($5d^96s^1$) would differentiate the small cluster structure of these two elements. Higher spin polarization than triplet is certainly possible for the ground state of platinum clusters.[3] Systematic theoretical investigations with DFT have been carried out on small platinum clusters Pt_n ($n = 1-4$[19] and $2-5$[22]). In the former work,[19] Pt_4 was found to have a triplet ground state with C_{2v} tetrahedron geometry. In the latter work,[22] only low-spin polarizations (singlet and triplet) have been considered for Pt_n, and the authors noted this limitation. Semiempirical MD simulations were performed on Pt_n clusters with $n = 2-21$,[15] and four isomers were located for Pt_7 with pentagonal bipyramid (PBP) as the global minimum. However, spin polarization was not considered in those calculations. Non-self-consistent Harris functional based calculations were performed for platinum clusters with cluster size up to six atoms[18] without any spin polarization. No detailed theoretical studies have been carried out for platinum clusters with a size larger than six atoms.

In this work, we present the DFT studies of structural and electronic properties of the Pt_7 cluster to locate its possible minima and its ground state. Comparisons with the well-studied Au_7 heptamer cluster are also made wherever possible. In recent years, there have been several DFT studies on the structure of neutral Au_7 cluster. In one paper of Zhao et al.,[4a] three isomers—PBP, capped "octahedron" (COh), and hexagon (HEX)—were studied, and the PBP was found to be the most stable. Both

* Corresponding author. Phone: 86-10-62558682. Fax: 86-10-62559373. E-mail: gemaofa@iccas.ac.cn.
[†] University of British Columbia.
[‡] Chinese Academy of Sciences.
[§] Kansai Advanced Research Center.
[||] University of Texas at Austin.

10.1021/jp0498365 CCC: $27.50
Published on Web 04/06/2004

TABLE 1: Comparison of the Calculated (with Gaussian Basis) and Experimental[a] Bond Lengths, Vibrational Frequencies, and Bond Energy of Pt_2 and Au_2

	bond length (Å)		vibrational frequency (cm^{-1})		bond energy (in eV)	
	calcd	expt	calcd	expt	calcd	expt
Au_2	2.551	2.473	167.1	190.9	2.04	2.31
Pt_2	2.386	2.333	222.9	222.5	3.29	3.14

[a] For Pt_2, see refs 9−11; for Au_2, see refs 5−7.

Häkkinen et al.[3a] and Zhao et al.[4b] also proposed a planar HEX structure. In the latest joint experimental and theoretical studies of Häkkinen et al.,[8] four isomers, edge-capped rhombus (ECR), edge-capped "square" (ECS), edge-capped pyramid (ECP), and W-like structure (W), were considered, and the ECR was found to be the most stable isomer. We studied all of these structures and considered other possible isomers. Vibrational frequency calculations of all the optimized structures have also been carried out to verify the nature of these stationary points (local minimum with no negative eigenvalue, transition state with one and only one negative eigenvalue, and high-order saddle point with more than one negative eigenvalue for Hessian).

II. Computational Method

DFT methods as implemented in Gaussian 98[25] have been used for the calculations of structures and harmonic frequencies of neutral gold and platinum clusters. We used the generalized gradient approximation (GGA) of Becke[26] and Perdew[27,28] for exchange and correlation functional (BPW) and employed the relativistic 19-electron Los Alamos National Laboratory (LANL2DZ) effective core pseudopotentials[29] with the basis sets (3s3p2d). The relativistic effect was found to be important to the modeling of gold clusters,[3b] and the relativistic effect is also very strong in Pt.[24] This method was applied to the theoretical studies of small platinum and gold hydrides and oxides.[23,30,31] For comparison, the calculations were also performed for the optimizations of these clusters with a plane-wave expansion method[32] employing scalar relativistic ultrasoft pseudopotentials[33] and the spin-polarized version of the generalized gradient approximation (GGA) for exchange and correlation.[34] Natural bond orbital (NBO)[35] analysis was carried out on the most stable isomers of Pt_7 and Au_7.

III. Results and Discussions

A. Pt_2 and Au_2. We begin with a discussion of neutral Pt_2 and Au_2 clusters. Table 1 shows the comparisons of the calculated (with the Gaussian basis) and experimental bond lengths, vibrational frequencies, and bond energy of Pt and Au dimers. We observe that the calculated results are in good agreement with experiment. The present method is better than the performance of PW91 exchange correlation with a double-ζ-plus-polarization set in platinum cluster modeling[19] in the vibrational frequency and bond energy predicitons. The good agreement with experiment validates BPW GGA with LANL2DZ in gold and platinum clusters modeling. The ground state of Pt_2 is triplet, and the gap between the highest occupied molecular orbital (β spin) and the lowest unoccupied molecular orbital (β spin) (HOMO−LUMO) is 0.3 eV. The triplet−singlet split of Pt_2 is 1.46 eV. The electronic configuration of Pt in ground-state Pt_2 is (core)$5d^{8.92}6s^{1.07}6p^{0.01}$ with two unpaired electrons in d_{xz} and d_{yz} orbitals (z is the bond axis), respectively, according to the NBO analysis. The ground state of gold dimer is singlet and the electronic configuration of Au in Au_2 is (core)-$6s^{1.04}5d^{9.94}6p^{0.02}$. The singlet−triplet split of the Au_2 is 2.02 eV.

TABLE 2: Relative Stability of Neutral Gold Heptamer Isomers Predicted by Using BPW with LANL2DZ Relativistic Pseudopotentials with Gaussian Basis Set and by Using Semirelativistic Ultrasoft Pseudopotentials with Plane-Wave Expansion

isomers	Gaussian[a]	ΔE (eV)	plane-wave ΔE (eV)	isomers	Gaussian[a]	ΔE (eV)	plane-wave ΔE (eV)
ECR	MIM	0.000	0.000	COh	TS	0.652	0.529
ECS	TS	0.090	0.114	ECP	TS	0.690	0.600
ECT	MIM	0.267	0.351	W	MIM	0.705	0.632
HEX	MIM	0.360	0.230	CP	SP	0.740	0.585
TCT	MIM	0.481	0.379	CTP	SP	0.833	0.710
PBP	MIM	0.520	0.416				

[a] MIN, minimum; TS, transition state; SP, higher order saddle point.

TABLE 3: Relative Stability of Isomers of Neutral Platinum Heptamer Predicted by Using BPW with LANL2DZ Relativistic Pseudopotentials with Gaussian Basis Set and by Using Semirelativistic Ultrasoft Pseudopotentials with Plane-Wave Expansion

isomers	Gaussian[a]		ΔE (eV)	plane-wave ΔE (eV)
CTP	quintet	MIM	0.000	0.000
	septet	MIM	0.007	0.053
	triplet	MIM	0.102	0.103
	nonet	MIM	0.394	0.311
	singlet	MIM	0.403	0.205
ECTB	triplet	MIM	0.162	0.213
	quintet	TS	0.314	
	singlet	MIM	0.536	0.267
FCTB	quintet	MIM	0.300	0.399
	triplet	MIM	0.308	0.408
	singlet	MIM	0.518	0.461
ECT	triplet	TS	0.322	
	quintet	SP	0.417	
COh	quintet	MIM	0.356	0.391
	septet	TS	0.379	
	triplet	MIM	0.390	0.488
TCT	triplet	MIM	0.543	0.074
	singlet	TS	0.882	0.864
PBP	quintet	TS	0.756	0.749
	septet	TS	0.781	0.427
	triplet	SP	0.916	0.947
	singlet	SP	1.219	0.866
ECR	triplet	SP	1.044	
	quintet	SP	1.262	
W	triplet	SP	2.044	
	quintet	SP	2.333	
	singlet	SP	2.486	
ECP	triplet	SP	2.132	
	quintet	SP	2.172	
	singlet	SP	3.408	
ECS	triplet	TS	2.288	
	quintet	SP	2.635	
	singlet	TS	2.845	
HEX	singlet	SP	2.516	

[a] MIN, minimum; TS, transition state; SP, higher order saddle point.

B. Au_7. There are 11 structures for Au_7 located with the LANL2DZ pseudopotential Gaussian calculations. The electronic configuration of Au is (core)$5d^{10}6s^1$. The closed shell structure in the 5d shell makes it difficult for the Au cluster to have a stable electronic state with high spin polarization[3b]. The ground state for Au_7 is doublet planar ECR, and the relative energies of Au_7 isomers to the ground state are listed in Table 2. The ECR is 0.90 eV (725 cm^{-1}) more stable than the second most stable stationary point ECS. ECS is a transition state according to DFT frequency calculations. In the anionic state, we found that ECS is the ground state and ECR is the second

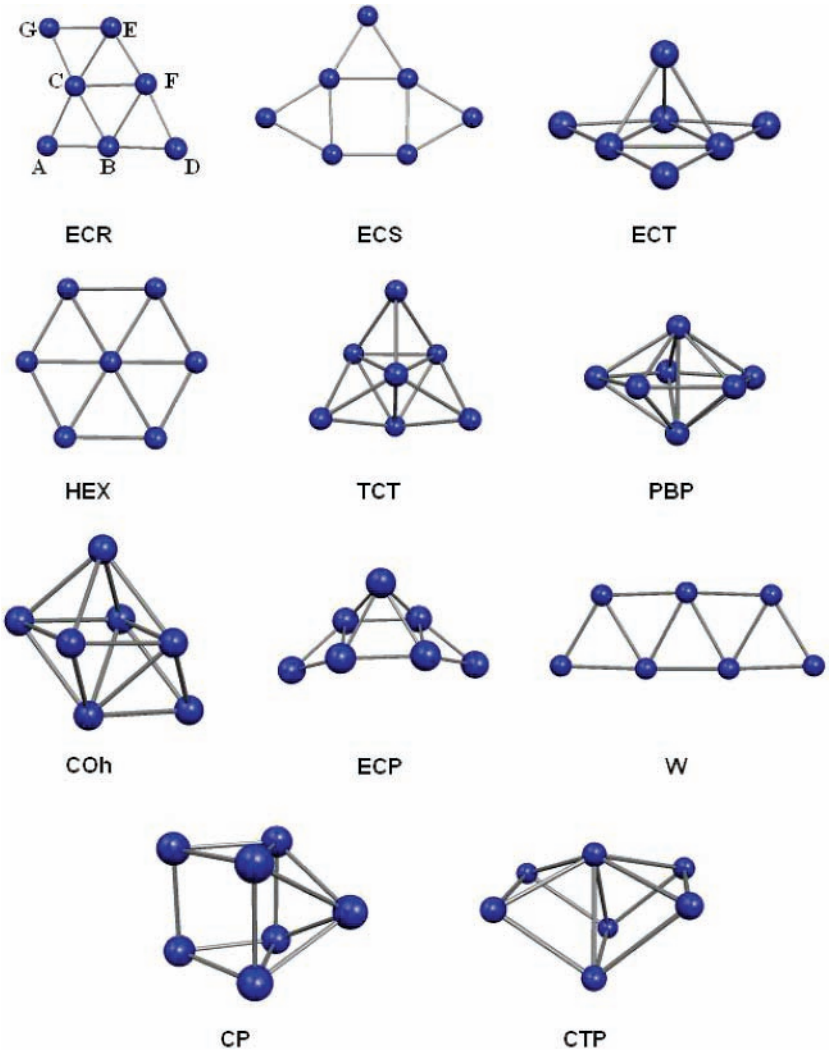

Figure 1. Structures of neutral gold heptamer clusters.

most stable structure in our calculation; this is in agreement with the previous theoretical result.[3b] Totally, six minima were located for Au_7, as shown in Figure 1. Among the six minima, edge-capped tetrahedron (ECT), tri-capped tetrahedron (TCT), and PBP are 3D structures and ECR, ECS, and W are planar. Our plane-wave calculations confirm the relative stability of Au_7 isomers predicted by the LANL2DZ pseudopotential. From the relative energies of the Au_7 isomers, one notes that Au_7 prefers a planar structure for its ground state. Anionic Au_7 cluster, Au_7^-, also prefers a planar ground state.[3b]

C. Pt_7. We searched the ground state of Pt_7 from singlet ($S = 0$) to nonet ($S = 4$). The ground state of Pt_7 is found to be a quintet state with four unpaired electrons with coupled tetragonal pyramid (CTP) geometry predicted by both the effective LANL2DZ relativistic core pseudopotentials and the semirelativistic ultrasoft pseudopotentials. All the relative energies of the isomers to the ground state of Pt_7 (CTP, quintet) are listed in Table 3 and the isomer geometries are shown in Figure 2. We start our discussion on the structures from the BPW with LANL2DZ relativistic core pseudopotentials calculations. The CTP structure of Pt_7 is similar to a complex of Dewar benzene with an oxygen atom lying above.[36] The platinum atom (G in Figure 2) above the Dewar benzene shaped Pt_6 in CTP Pt_7 has shorter bond distances to the four boat-end platinum atoms (A, B, D, and F) than the bond distances to the two bottom platinum atoms (C and E). Among the five electronic states of CTP Pt_7 considered, the septet is the first excited state and it is only 57 cm^{-1} above the quintet CTP Pt_7. This energy difference is below the Pt heptamer vibrational temperature.[37] The quintet CTP Pt_7 could easily be excited to the septet CTP Pt_7 due to the relativistic effect and spin−orbital coupling.[38] Triplet is the second excited state, and it is 0.102 eV above the quintet. Within the accuracy of the DFT prediction, the quintet and septet CTP Pt_7 are energetically degenerate. The three electronic states (quintet, septet, and triplet) of CTP are also the lowest electronic states among all the conformations of Pt_7 studied. Among all the structures studied, quintet CTP is the global minimum for Pt_7. The singlet of CTP is the highest electronic state among the five states studied for CTP Pt_7 and nonet is the second highest one. The structures of the CTP Pt_7 in all the five electronic state are minima.

Three stationary points with edge-capped trigonal bipyramid (ECTB) shape were located, one in triplet, one in quintet, and the other one in singlet. The energy of the triplet ECTB is only higher than the energy of the CTP quintet, septet, and triplet. Within the face-capped trigonal bipyramid (FCTB) shape, only quintet, triplet, and singlet states are minima. The septet state of FCTB converged to distorted CTP (minimum) structure, and its energy is 0.172 eV (0.150 eV in plane-wave calculations) higher than that of the ground-state Pt_7. Pt_7 has no minimum for the ECT structure. The triplet and quintet of COh structures are also minima. For the TCT structure, the triplet Pt_7 is a minimum. Septet TCT converges to a distorted CTP (minimum) structure. Quintet TCT also converges to a distorted CTP

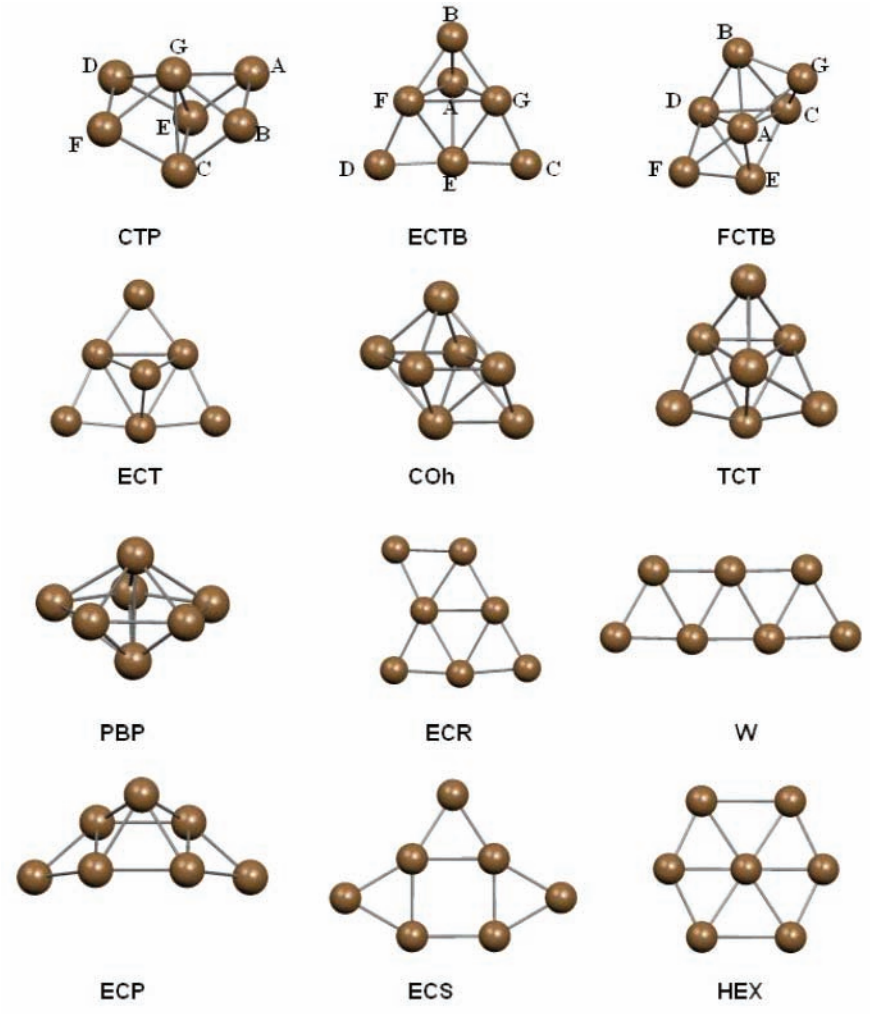

Figure 2. Structures of neutral platinum heptamer clusters

minimum, being 0.224 eV (0.040 eV in plane-wave calculations) higher than the ground state. There is no minimum located for PBP, ECR, W, ECP, ECS, and HEX. All the stationary points located with these geometries (PBP, ECR, W, ECP, ECS, and HEX) are found to have much higher energies than the CTP ground state. The singlet state of ECT, COh, and ECR isomers do not converge in our DFT calculations. The energies of quintet and septet CTP are so close that these two electronic states are nearly degenerate. No planar minimum has been located for Pt_7. The FCTB and ECTB structures of Pt_7 do not present themselves in Au_7 clusters.

For Pt_7 clusters, only the local minima and PBP structures were considered for the plane-wave calculations. Essentially, plane-wave calculations give similar order of relative stability for Pt_7 clusters as that predicted by the LANL2DZ pseudopotential calculations. A notable exception is that plane-wave calculations predicted triplet TCT, the third most stable structure, while the third most stable structure in LANL2DZ pseudopotential calculations is the triplet CTP, and it is the fourth most stable in plane-wave calculations. This may be due to the semirelativistic ultrasoft pseudopotentials[33] used in our plane-wave based calculations for the structural optimizations, and such a small energy difference is beyond the predicting capability of present DFT methods,[26,32] so no conclusive remark about the relative stability predicted by present DFT methods for these isomers could be reached.

D. Electronic Configurations, NBO Analysis, and Density of States (DOS). Metal clusters, especially of a transition metal that has incomplete d shell electrons, are particularly useful in catalysis. The reactivity of the metal clusters, which stems from the electronic structure of the metal clusters, depends on the number of atoms and the arrangement of the atoms in the clusters. For metal clusters, there exists a size-induced metal−insulator transition (SIMIT).[49] The energy level spacing of metal clusters gets discrete as the cluster size gets small, thus resulting in a large band gap (HOMO−LUMO gap for small clusters). The electronic configuration gives the detailed electronic structure for a system and sheds light on the reactivity of the system. The DOS of a cluster gives an overall picture for the cluster electronic structure. It provides the detailed structure for the subshell electrons in a cluster (analogue of a band structure for the corresponding bulk system). The band structures close to the HOMO and LUMO (the Fermi energy level for the bulk systems) have particular influence on the chemical reactivity of metal cluster.

1. Au_7. Only the ground state of Au_7 (ECR) was analyzed for its electronic structure. The discreteness of the DOS is evident from Figure 3. The intense peaks of DOS of the ECR Au_7 distribute from −9.0 to −6.0 eV; essentially three bands lie close to one another within this energy range. The bonding of the ECR Au_7 is clearly reflected from its occupied molecular orbitals (as shown in Figure 3). The σ bonds formed by the 5d atomic orbitals contribute to the bonding in the ECR Au_7. The molecular obtials close to the HOMO are non- or antibonding orbitals and they are mainly 5d6s hybridized. Due to the electronic configuration of the Au atom ($5d^{10}6s^1$), the bonding

TABLE 4: Electronic Configurations of the Lowest Stationary Point of the Pt_7 Cluster and the Ground State of Au_7[a]

atom	ECR Au_7 doublet	CTP Pt_7 quintet	CTP Pt_7 septet
A	5d(9.89)6s(1.14)6p(0.01)	5d(9.08)6s(0.94)6p(0.03)6d(0.01)	5d(9.11)6s(0.97)6p(0.02)6d(0.01)
B	5d(9.87)6s(0.98)6p(0.05)6d(0.01)7p(0.01)	5d(9.08)6s(0.94)6p(0.03)6d(0.01)	5d(9.09)6s(0.93)6p(0.03)6d(0.01)
C	5d(9.86)6s(0.98)6p(0.07)6d(0.01)	5d(9.06)6s(0.84)6p(0.04)7p(0.01)	5d(9.04)6s(0.89)6p(0.03)7p(0.01)
D	5d(9.89)6s(1.18)6p(0.01)	5d(9.08)6s(0.94)6p(0.03)6d(0.01)	5d(9.11)6s(0.97)6p(0.02)6d(0.01)
E	5d(9.88)6s(1.05)6p(0.03)	5d(9.06)6s(0.84)6p(0.04)7p(0.01)	5d(8.96)6s(0.86)6p(0.05)7p(0.01)
F	5d(9.91)6s(1.05)6p(0.03)6d(0.01)7p(0.01)	5d(9.08)6s(0.95)6p(0.03)6d(0.01)	5d(9.09)6s(0.93)6p(0.03)6d(0.01)
G	5d(9.91)6s(1.15)6p(0.01)	5d(9.14)6s(0.69)6p(0.06)6d(0.01)7p(0.01)	5d(9.07)6s(0.71)6p(0.07)6d(0.01)7p(0.01)

atom	CTP Pt_7 triplet	ECTB Pt_7 triplet	FCTB Pt_7 quintet
A	5d(9.08)6s(0.95)6p(0.02)6d(0.01)	5d(9.10)6s(0.62)6p(0.04)6d(0.01)	5d(9.17)6s(0.70)6p(0.05)6d(0.01)7p(0.01)
B	5d(9.06)6s(0.96)6p(0.03)6d(0.01)	5d(9.01)6s(1.06)6p(0.03)6d(0.01)	5d(9.18)6s(0.75)6p(0.03)6d(0.01)
C	5d(9.06)6s(0.81)6p(0.04)7p(0.01)	5d(8.98)6s(1.15)6p(0.01)6d(0.01)	5d(9.16)6s(0.74)6p(0.05)6d(0.01)7p(0.01)
D	5d(9.09)6s(0.92)6p(0.03)6d(0.01)	5d(8.98)6s(1.15)6p(0.01)6d(0.01)	5d(9.19)6s(0.72)6p(0.05)6d(0.01)7p(0.01)
E	5d(9.09)6s(0.82)6p(0.03)7p(0.01)	5d(8.97)6s(0.94)6p(0.05)6d(0.01)7p(0.01)	5d(9.19)6s(0.75)6p(0.03)6d(0.01)
F	5d(9.06)6s(0.99)6p(0.03)6d(0.01)	5d(9.03)6s(0.85)6p(0.04)6d(0.01)7p(0.01)	5d(9.13)6s(0.95)6p(0.03)6d(0.01)
G	5d(9.13)6s(0.69)6p(0.06)6d(0.01)7p(0.01)	5d(9.03)6s(0.85)6p(0.04)6d(0.01)7p(0.01)	5d(9.14)6s(0.92)6p(0.03)6d(0.01)

[a] The core electrons are not shown. The labels of atoms in each structure are shown in Figures 1 and 2.

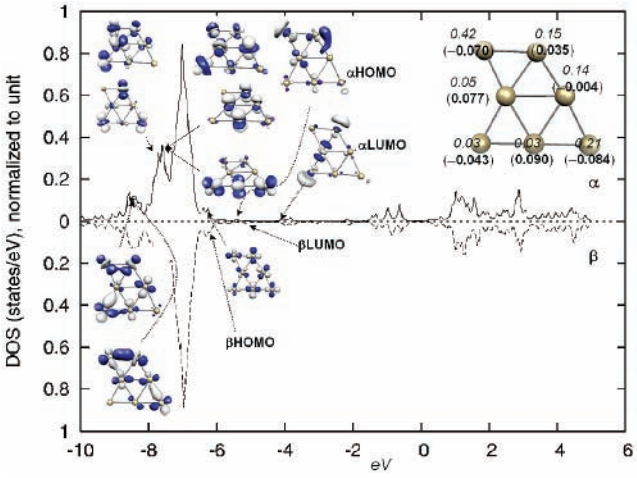

Figure 3. The α and β spin density of states of the doublet ECR Au_7. The net spin charges and the natural atomic orbital partial charges (in parentheses) are also shown.

contribution from 5d in Au_7 is limited. This limited bonding contribution from 5d in Au_7 is also manifested by the electronic configuration of the ECR Au_7 (as listed in Table 4), in which partial intra- and interatomic charges transfer occur from 5d to 6s. The 5d subshells are almost fully occupied. The different spin densities and the natural partial charges of Au atoms in the ECR Au_7 (in Figure 3) indicate their different chemical reactivity.

2. Pt_7. Referring to atomic labels in Figure 2 for the Pt_7 ground-state structure, quintet CTP Pt_7, the electronic configuration shows that the apex (labeled G) has large intra-atomic charge transfer from 6s to 5d and 6p (even to 6d and 7s). The middle Pt pair atoms (C and E) in quintet CTP Pt_7 have intra-atomic charge transfer from 6s to 5d, 6p, and 7p. All the three atoms have interatomic charge transfer to the other four Pt atoms (A, B, D, and F). The charge transfer could also be seen from the natural partial charge analysis, as shown in Figure 4a. Atoms C, E, and G have positive charges, while A, B, D, and F have negative charges. The intra-atomic charges transfer from 6s to 5d and 6p take place on all seven atoms in the quintet CTP Pt_7. The Pt dimer (Pt_2) has opposite intra-atomic charge transfer (from 5d to 6s). The four unpaired electrons mainly distribute on atoms A, B, C, D, E, and F, the atom G has very little net spin density. According to the electronic configuration and natural partial charge analysis, the quintet CTP Pt_7 has nearly symmetric (C_{2v}) structure. Among the atoms A, B, C, D, E, and F in the quintet CTP Pt_7, atoms C and E have the highest net spin density and negative charges. These two atoms also have the longest distances to G, the apex.[40a]

The second most stable structure, the septet CTP Pt_7, has slightly different electronic structure from that of the quintet CTP Pt_7 (Figure 4b). The intra-atomic charge transfer (from 6s to 5d, 6p, 6d, and 7p) is less in the septet than in the quintet CTP Pt_7 according to the natural electronic configuration analysis. The interatomic charge transfer is stronger in the septet CTP Pt_7, as manifested by the natural electronic configurations of atoms and the natural partial charge analysis. The apex (atom G) has the largest deviation for its electronic configuration from that in Pt_2, which is the same case for the quintet CTP Pt_7. In the quintet CTP Pt_7, both atoms C and E have large charge transfer to A, B, D, and F. In the septet CTP Pt_7, atom E has much stronger charge transfer to A, B, D, and F than that from the atom C to A, B, D, and F; this is revealed by unbalanced natural partial charges on these two atoms (E, 0.122; C, 0.038). The unbalanced charge distribution (and net spin distribution) is also reflected between atoms A and B, and D and F, thus resulting in a distorted geometry of the septet CTP Pt_7.[40b] Large charge transfer occurs from atoms E and G to atoms A and D in the septet CTP Pt_7. In the septet CTP Pt_7, atom E has the largest net spin density and atom G has the smallest one.

The electronic configurations for all the five lowest stationary points of Pt_7 cluster are displayed in Table 4. The triplet CTP Pt_7 has very similar electronic configurations to that of the quintet CTP Pt_7 (Figure 4c). It also has similar geometry to that of the quintet CTP Pt_7.[40c] It is interesting, however, that the triplet CTP Pt_7 has different pattern of charge and net spin distribution from that of the quintet CTP Pt_7. The atom pairs in the triplet CTP Pt_7 (A and B, C and E, D and F) have uneven charge and net spin density on the two atoms of each atom pair. Atoms A and G in the triplet CTP Pt_7 have even net β spin density. The NBO analysis clearly indicates the excited-state nature of the triplet CTP Pt_7.

The triplet ECTB Pt_7 is the forth most stable conformation. It is 0.06 eV above the triplet CTP Pt_7. The geometry of the triplet ECTB Pt_7 has C_s symmetry. Large interatomic [from A, F and G (6s) to B, C, and D (5d)] and intra-atomic (A, from 6s to 5d) charge transfer occurs in the triplet ECTB Pt_7 (Figure 5a). Interatomic charge transfer occurs between the three apexes of the triangle (BCD) and the remaining four Pt atoms, and these charge transfers are from the latter four atoms to BCD. The interatomic charge transfer is manifested by the natural partial charge analysis. Even larger intra- and interatomic charge

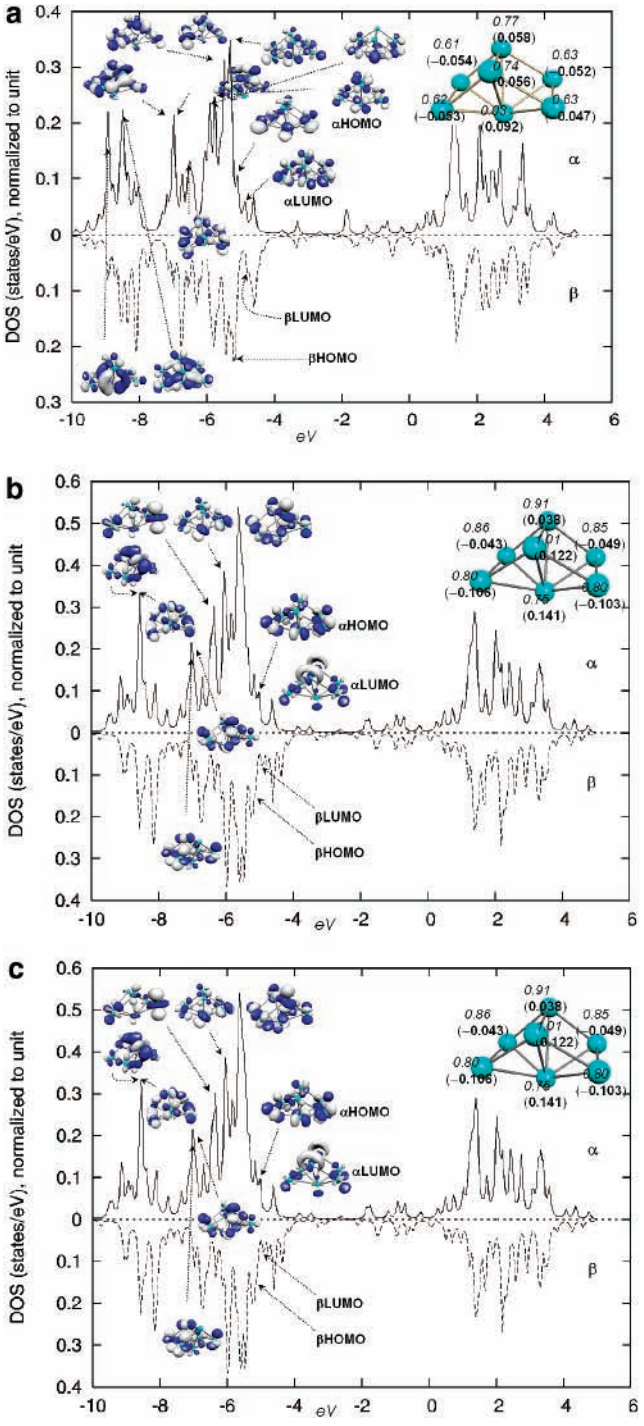

Figure 4. (a) The α and β spin density of states of quintet CTP Pt_7 cluster. The net spin charges and the natural atomic orbital partial charges (in parentheses) are also shown. (b) The α and β spin density of states of septet CTP Pt_7 cluster. The net spin charges and the natural atomic orbital partial charges (in parentheses) are also shown. (c) The α and β spin density of states of triplet CTP Pt_7 cluster. The net spin charges and the natural atomic orbital partial charges (in parentheses) are also shown.

transfer (compared to those in the triplet ECTB Pt_7) occurs in the FCTB quintet Pt_7, as revealed by its electronic configuration. The natural partial charges of the FCTB quintet Pt_7 are displayed in Figure 5b and the partial charges manifest large intra- and interatomic charge transfer. The net spin charge distributions on the ECFTB triplet Pt_7 and the FCTB quintet Pt_7 are relatively even. Overall, the charge transfer is from 6s to 5d, 6p, and 7p in all the Pt_7 conformations investigated above.

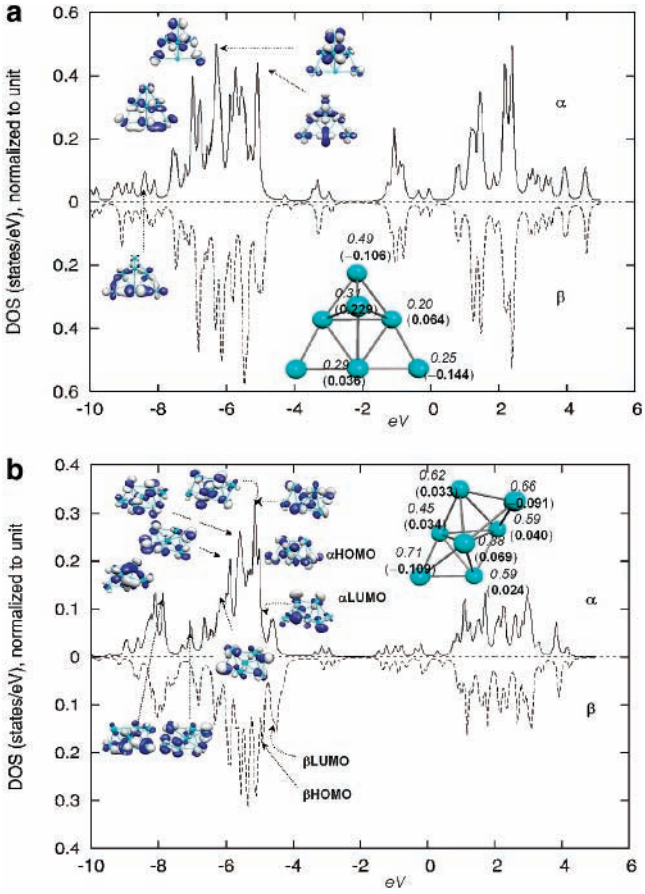

Figure 5. (a) The α and β spin density of states of the triplet ECTB Pt_7 cluster. The net spin charges and the natural atomic orbital partial charges (in parentheses) are also shown. (b) The α and β spin density of states of the quintet FCTB Pt_7 cluster. The net spin charges and the natural atomic orbital partial charges (in parentheses) are also shown.

Figures 4 and 5 depict the α spin and the β spin DOS of the first five most stable conformations of Pt_7. Molecular orbitals corresponding to the intense peaks of the α spin are also drawn in these figures. The β spin molecular orbitals are similar to the α spin molecular orbitals. For the CTP quintet Pt_7, the overall shape of the α spin DOS is similar to that of β spin DOS, except that the α spin DOS shifts to a low-energy region. According to the molecular orbital analysis, the HOMO and the orbital immediately below the HOMO (from −4.0 to −6.0 eV) mainly consist of 5d and 6s atomic orbitals. The occupied orbitals below −6.0 eV consist of contributions from 5d atomic orbitals. The HOMO and the molecular orbitals closely below the HOMO (from −4.0 to −7.0 eV) mainly are antibonding or nonbonding orbitals. The molecular orbitals below −7.0 eV are bonding orbitals. The α spin molecular orbitals have the HOMO and the LUMO with a small HOMO−LUMO gap (0.21 eV). From −4.0 eV to the Fermi energy level, the DOS of the CTP quintet Pt_7 are sparse and discrete. Within this energy range (−4.0 eV to the Fermi energy level), the molecular orbitals are mainly contributed from 6s and 6p (and a small amount of 5d) atomic orbitals. The higher energy virtual molecular orbitals consist of contribution from 6s and 6p atomic orbitals, thus resulting in sp hybridization for the molecular orbitals with energy from the Fermi energy to 2.0 eV [the partial density of state (PDOS) for the investigated systems are provided in the Supporting Information]. We also did PDOS analysis with plane-wave calculations and got similar results (figures not shown).

The geometric change from the quintet CTP Pt_7 to the septet CTP Pt_7 renders the change of DOS and electronic structure in

the septet CTP Pt_7, though the energy of the septet CTP Pt_7 is very close to that of the quintet CTP Pt_7. The change is reflected in the DOS shape and the molecular orbital shape, as depicted in Figure 4b. For example, in the DOS, there is a gap (about 0.6 eV) between the bands from −4.0 to −7.0 eV and the bands from −7.0 to −9.0 eV in the quintet CTP Pt_7; this gap is smaller in the septet CTP Pt_7 DOS (about 0.3 eV). The septet CTP Pt_7 has an α spin HOMO and a β spin LUMO with a HOMO−LUMO gap of 0.12 eV; this HOMO−LUMO gap is smaller than that of quintet CTP Pt_7. The molecular orbitals of the septet CTP Pt_7 have similar components as those of the quintet CTP Pt_7; i.e., 5d (and 6s) atomic orbitals contribute to the bonding orbitals and nonbonding occupied orbitals above −10.0 eV, and the virtual orbitals have contributions from 6s and 6p atomic orbitals.

The triplet CTP Pt_7 has similar DOS shape and molecular orbital shape as those of the quintet CTP Pt_7. The (β spin) HOMO−(α spin) LUMO gap (0.07 eV) of triplet CTP Pt_7 is smaller than that of both the quintet and the septet CTP Pt_7.

The DOS shape of the triplet ECTB Pt_7 is different from that of the CTP Pt_7, while the DOS shape of the quintet FCTB Pt_7 is similar to that of the CTP Pt_7. This shape difference of the DOS of the triplet ECTB Pt_7 from the other DOSs is reflected by its geometry, and the geometry difference renders a different electronic structure. Except for the atom A in the triplet ECTB Pt_7, the other six Pt atoms are nearly in one plane.

IV. Conclusions

In conclusion, we have studied the structural, energetic, and electronic properties of the platinum and gold heptamers by using density functional calculations employing relativistic effective core pseudopotentials with Gaussian basis and plane-wave pseudopotential. We found that the Pt_7 cluster favors 3D geometries, and a 2D local minimum is not located. The most stable isomer of Au_7 is found to be a planar 2D structure, and an ECT structure is found to be the most stable 3D local minimum, which is not found for other transition-metal heptamers. The DOS analysis suggests that the preference of the 3D structure for Pt_7 is due to the large bonding contribution from the 5d atomic orbitals. It is also found that the ground state of the Pt_7 cluster is a CTP structure with a quintet state at the DFT level of theory. The quintet CTP Pt_7 is nearly degenerate with the septet CTP Pt_7. The PBP structure, which is the global minimum in molecular dynamics (MD) simulation,[15] is not a local minimum in the DFT investigation.

Acknowledgment. Prof. M. F. Ge would like to thank the foundation of the Chinese Academy of Sciences (Hundred Persons Talents) and Japan Society for the Promotion of Science (JSPS) for financial support. Dr. B. R. Sahu would like to thank the Texas Advanced Computing Center (TAAC), University of Texas at Austin, for the computational support.

Supporting Information Available: Optimized Cartesian coordinates of all the structures at the level of BPW91/LANL2DZ, DOS, and PDOS of the five most stable Pt_7 conformations and Au_7 ECR from Gaussian calculations. This material is available free of charge via the Internet at http://pubs.acs.org.

References and Notes

(1) (a) Mirkin, C. A.; Letsinger, R. L.; Mucic, R. C.; Storhoff, J. J. *Nature* **1996**, *382*, 607. (b) Hong B. H.; Bae S. C.; Lee C. W.; Jeong S.; Kim K. S. *Science* **2001**, *294*, 348. (c) Haruta, M. *Catal. Today* **1997**, *36*, 153. (d) Häkkinen, H.; Abbet, S.; Sanchez, A.; Heiz, U.; Landman, U. *Angew. Chem. Int. Ed.* **2003**, *42*, 1297.

(2) Taylor, K.; Hall, C. P.; Cheshnovsky, O.; Smally, R. *J Chem. Phys.* **1992**, *96*, 3319.

(3) (a) Häkkinen, H.; Landman, U. *Phys. Rev. B* **2000**, *62*, R2287. (b) Häkkinen, H.; Moseler, M.; Landman, U. *Phys. Rev. Lett.* **2002**, *89*, 033401.

(4) (a)Wang, J.; Wang, G.; Zhao, J. *Phys. Rev. B* **2002**, *66*, 035418. (b) Zhao, J.; Yang, J.; Hou, J. G. *Phys. Rev. B* **2003**, *67*, 085404.

(5) Simard, B.; Hackett, P. A. *J. Mol. Spectrosc.* **1990**, *142*, 310.

(6) Morse, M. D. *Chem. Rev.* **1986**, *86*, 1049.

(7) James, A. M.; Kowalczyk, P.; Simard, B.; Pinegar, J. C.; Morse, M. D. *J. Mol. Spectrosc.* **1994**, *168*, 248.

(8) Häkkinen, H.; Yoon, B.; Landman, U.; Li, X.; Zhai, H. J.; Wang, L. S. *J. Phys. Chem. A* **2003**, *107*, 6168.

(9) Airola, M. B.; Morse, M. D. *J. Chem. Phys.* **2002**, *116*, 1313.

(10) Fabbi, J. C.; Langenberg, J. D.; Costello, Q. D.; Morse, M. D.; Karlsson, L. *J. Chem. Phys.* **2001**, *115*, 7543.

(11) Taylor, S.; Lemire, G. W.; Hamrick, Y. M.; Fu, Z.; Morse, M. D. *J. Chem. Phys.* **1988**, *89*, 5517.

(12) Jansson, K.; Scullman, R. *J. Mol. Spectrosc.* **1976**, *61*, 299.

(13) Gupta, S. K.; Nappi, B. M.; Gingerich, K. A. *Inorg. Chem.* **1981**, *20*, 966.

(14) (a)Ho, J.; Polak, M. L.; Ervin, K. M.; Lineberger, W. C. *J. Chem. Phys.* **1993**, *99*, 8542.(b) Ervin, K. M.; Ho, J.; Lineberger, W. C. *J. Chem. Phys.* **1988**, *89*, 4514. (c) Grushow, A.; Ervin, K. M. *J. Chem. Phys.* **1997**, *106*, 9580.

(15) Sebetci, A.; Güvenç, Z. B. *Surf. Sci.* **2003**, *525*, 66.

(16) Rodeja, J. G.; Rey, C.; Galleo, L. J.; Alonso, J. A. *Phys. Rev. B* **1994**, *49*, 8495.

(17) (a) Balasubramanian, K. *J. Chem. Phys.* **1987**, *84*, 6573. (b) Dai, D.; Balasubramanian, K. *J. Chem. Phys.* **1995**, *103*, 648. (c) Majumdar, D.; Dai, D.; Balasubramanian, K. *J. Chem. Phys.* **2000**, *113*, 7919. (d) Majumdar, D.; Dai, D.; Balasubramanian, K. *J. Chem. Phys.* **2000**, *113*, 7928.

(18) Yang, S. H.; Drabold, D. A.; Adams, J. B.; Ordejon, P.; Glassford, K. *J. Phys.: Condens. Matter* **1997**, *9*, L39.

(19) (a) Fortunelli, A. *J. Mol. Struct. (THEOCHEM)* **1999**, *493*, 233. The predicted vibrational frequency for Pt_2 is 231 cm^{-1}, and the bond energy of Pt_2 is 3.70 eV in this work. (b) Apra, E.; Fortunelli, A. *J. Mol. Struct. (THEOCHEM)* **2000**, *502*, 251.

(20) Varga, S.; Fricke, B.; Nakamatsu, H.; Mukoyama, T.; Anton, J.; Geschke, D.; Heitmann, A.; Engel, E.; Başt ğ, T. J. Chem. Phys. **2000**, *112*, 3499.

(21) Cui, Q.; Musaev, D. G.; Morokuma, K. *J. Chem. Phys.* **1998**, *108*, 8418.

(22) Grönbeck, H.; Andreoni, W. *Chem. Phys.* **2000**, *262*, 1.

(23) Li, T.; Balbuena, P. B. *J. Phys. Chem. B* **2001**, *105*, 9943.

(24) Pyykkö, P. *Chem. Rev.* **1988**, *88*, 563.

(25) *Gaussian 98*, revision A.7; Gaussian, Inc.: Pittsburgh, PA, 1998 (www.Gaussian.com).

(26) Becke, A. D. *Phys. Rev. A* **1988**, *38*, 3098.

(27) Perdew, J. P.; Chevary, J. A.; Vosko, S. H.; Jackson, K. A.; Pederson, M. R.; Singh, D. J.; Fiolhais, C. *Phys. Rev. B* **1992**, *46*, 6671.

(28) Perdew, J. P.; Burke, K.; Wang, Y. *Phys. Rev. B* **1996**, *54*, 16533.

(29) Hay, P. J.; Wadt, W. R. *J. Chem. Phys.* **1985**, *82*, 299.

(30) Wang, X.; Andrews, L. *J. Phys. Chem. A* **2001**, *105*, 5812.

(31) Andrews, L.; Wang, X.; Manceron, L. *J. Chem. Phys.* **2001**, *114*, 1559.

(32) Kresse, G.; Furthmler, J. *Comput. Mater. Sci.* **1996**, *6*, 15.

(33) Vanderbilt, D. *Phys. Rev. B* **1990**, *41*, 7892.

(34) Perdew, J. P.; Wang, Y. *Phys. Rev. B* **1992**, *45*, 13244.

(35) Carpenter, J. E.; Weinhold, F. *J. Mol. Struct. (THEOCHEM)* **1988**, *169*, 41.

(36) Tian, W. Q. Ph.D. thesis, University of Guelph, 2001.

(37) The vibrational temperature of an isolated polyatomic molecule could be defined as an average over all the vibration modes of the molecule. For example, see: Collings, B. A.; Amrein, A. H.; Rayner, D. M.; Hackett, P. A. *J. Chem. Phys.* **1993**, *99*, 4174.

(38) Balasubramaniat, K. *J. Chem. Phys.* **1991**, *94*, 1253.

(39) Johnston, R. L. *Atomic and Molecular Clusters*; Taylor & Francis: London, 2002.

(40) (a) Bond distances in quintet CTP Pt_7: R_{AB}, 2.603 Å; R_{AE}, 2.586 Å; R_{AG}, 2.624 Å; R_{BC}, 2.585 Å; R_{BG}, 2.624 Å; R_{CE}, 2.641 Å; R_{CF}, 2.586 Å; R_{CG}, 2.898 Å; R_{DE}, 2.586 Å; R_{DF}, 2.603 Å; R_{DG}, 2.625 Å; R_{EG}, 2.895 Å. (b) Bond distances in septet CTP Pt_7: R_{AB}, 2.616 Å; R_{AE}, 2.591 Å; R_{AG}, 2.723 Å; R_{BC}, 2.583 Å; R_{BG}, 2.655 Å; R_{CE}, 2.643 Å; R_{CF}, 2.583 Å; R_{CG}, 2.969 Å; R_{DE}, 2.592 Å; R_{DF}, 2.616 Å; R_{DG}, 2.723 Å; R_{EG}, 2.611 Å. (c) Bond distances in triplet CTP Pt_7: R_{AB}, 2.613 Å; R_{AE}, 2.588 Å; R_{AG}, 2.625 Å; R_{BC}, 2.588 Å; R_{BG}, 2.624 Å; R_{CE}, 2.634 Å; R_{CF}, 2.590 Å; R_{CG}, 2.900 Å; R_{DE}, 2.590 Å; R_{DF}, 2.588 Å; R_{DG}, 2.633 Å; R_{EG}, 2.896 Å.